# Polarity Propagation in the InSb/$\alpha$-Sn/InSb Heterostructure

Hiroo Omi,[1] Hideaki Saito,[1,*] and Toshiaki Osaka[1,2]
[1]*Department of Materials Science and Engineering, Waseda University, Shinjuku-ku, Tokyo 169, Japan*
[2]*Kagami Memorial Laboratory for Materials Science and Technology, Waseda University, Nishiwaseda, Shinjuku-ku, Tokyo 169, Japan*

(Received 4 October 1993)

Films of InSb{111}*A*,*B* grown on $\alpha$-Sn(111)/InSb{111}*A*,*B* by molecular beam epitaxy behave as if the polarity of their surfaces could receive that of the initial InSb substrates. InSb on $\alpha$-Sn(111)/InSb(111)*B* alternates the surface polarity with $\alpha$-Sn thickness. Below 5 bilayers (BL) $\alpha$-Sn, the growing InSb exhibits the *B* type of surface composed of Sb and beyond 5 BL it changes toward the *A* type. This is due to Sb segregation from the initial InSb(111)*B* substrate to the $\alpha$-Sn surface. On the other hand, InSb on $\alpha$-Sn(111)/InSb(111)*A* always grows with the *A*-type surface via formation of the intermixing layers of $(\mathrm{In}_x\mathrm{Sn}_{1-x})$Sb, decreasing the value of $x$ with increasing InSb thickness.

PACS numbers: 68.65.+g, 68.55.Bd, 82.65.Fr

Recent epitaxial growth techniques such as molecular beam epitaxy and metal-organic chemical vapor deposition have enabled us to fabricate a well-controlled heterostructure at an atomic scale. However, in order to fabricate desirable heterostructures, it is necessary to select a pair of as closely lattice matched materials as possible. The system of $\alpha$-Sn/InSb is typical of such a pair (lattice mismatch $\approx 0.14\%$). $\alpha$-Sn ($a = 6.489$ Å) is a nonpolar semiconductor and has a band gap nearly equal to zero (0.08 eV at 300 K), while InSb ($a = 6.4798$ Å) is a polar semiconductor and has a wider band gap (0.17 eV at 300 K). Thus, if electrons in the $\alpha$-Sn could be two-dimensionally confined by fabricating a heterostructure of InSb/$\alpha$-Sn/InSb, this system might have a great potential for a far-infrared laser.

The following information has already been established: (1) The surface structures of InSb{111}, a knowledge of which is indispensable for preparing a high-quality interface of the heterostructure, have been well established: for InSb(111)*A*-(2×2) the vacancy buckling model [1] and for InSb(111)*B*-(2×2) the Sb-trimer model [2]. (2) On the InSb{111} substrates, films of $\alpha$-Sn epitaxially grow with a biatomic layer-by-layer mode on InSb(111)*A* and with a more complicated layer-like mode on InSb(111)*B*, being accompanied by segregation of Sb [3] (details of which will be evidenced in this Letter), and they are stable even at temperatures much higher than 13.2 °C [4], but $\alpha$-Sn is usually unstable above this temperature.

In this Letter we report that the polar-nonpolar heterostructure of InSb/$\alpha$-Sn/InSb has been for the first time fabricated. Surprisingly, films of InSb grown epitaxially on $\alpha$-Sn(111)/InSb(111)*B* can alternate polarity of their surfaces with a film thickness of $\alpha$-Sn. For the thick [$>5$ bilayers (BL)] growth of InSb on $\alpha$-Sn(111)/InSb(111)*A* there always exists the *A*-type surface. Reflection high energy electron diffraction (RHEED), Auger electron spectroscopy (AES), and electron energy loss spectroscopy (EELS) have been used to identify the polar surfaces of the as-grown InSb films.

The experiments were performed in the molecular beam epitaxy system equipped with an electron gun for RHEED experiments and a cylindrical mirror analyzer with an integral gun for AES and EELS experiments. The substrates used in this work are (111)*A* and (111)*B* oriented InSb (nondoped). Details of the surface cleaning procedures have been described elsewhere [3]. High purity (99.9999%) Sn was evaporated onto the InSb{111} substrates at room temperature with a rate of $9\times10^{12}$ atoms/cm$^2$s, corresponding to 1 monolayer/min. Once films of $\alpha$-Sn reached a given thickness, the substrate was raised up to temperatures high enough to epitaxially grow InSb on it. Subsequently, films of InSb were epitaxially grown on the $\alpha$-Sn(111)/InSb{111} substrates with Sb$_4$/In flux ratios ranging from 3.2 to 4.8. The ultimate pressure and the pressure during evaporation were $3\times10^{-10}$ and $6\times10^{-9}$ Torr, respectively. Changes in surface structures of the InSb films were observed by RHEED. AES measurements were performed with the first derivative mode at a primary beam energy of 2 kV and at a total electron current of 1.0 $\mu$A. EELS spectra were taken with a primary electron beam of 80–400 eV and were recorded in the second derivative mode.

The surfaces of the InSb films grown epitaxially on the $\alpha$-Sn(111)($\theta$=3 BL)/InSb(111)*B* substrate at 200 °C under In-rich and Sb-rich conditions exhibited the (3×3) and the (2×2) reconstruction, respectively. Shown in Fig. 1(a) is the RHEED pattern for the (3×3) surface reconstruction which emerges on the InSb(111)*B* surface grown under the In-rich condition only. These results are also confirmed by the AES analysis. Table I shows the AES peak height ratios for the reconstructed surfaces compared to those for the homoepitaxially treated InSb(111)*B* substrate with the same surface reconstruction as the as-grown film surface. This table is indicative of a good agreement between the ratios for the Sb-stabilized surface. The appreciable deviation of those for the In-stabilized surface is likely due to the fact that In

0031-9007/94/72(16)/2596(4)$06.00

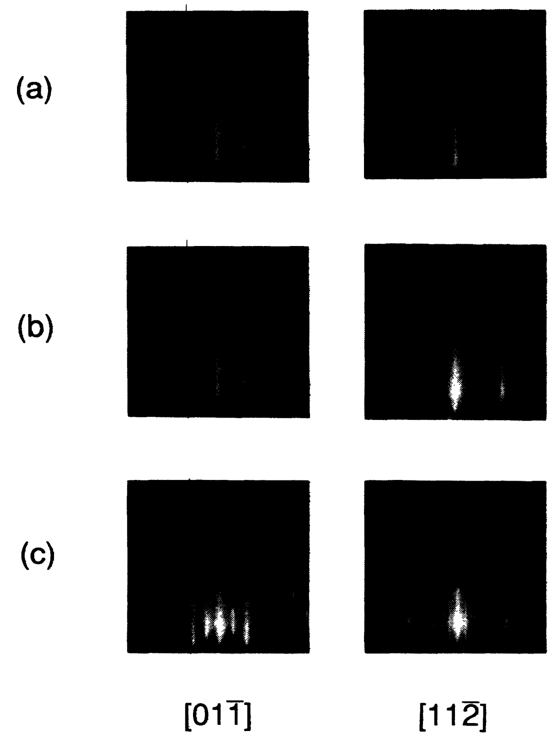

FIG. 1. RHEED patterns obtained by deposition of In and $Sb_4$ fluxes onto the $\alpha$-Sn(111)/InSb{111}*A*,*B*-(2×2) substrates at 200 °C. (a) The (3×3) reconstruction showing a *B*-type surface formed under the In-rich condition. (b) The (2×2) structure corresponding to the intermixing layers of $(In_xSn_{1-x})Sb$ formed under the Sb-rich condition. (c) The (2×6) reconstruction for an *A*-type surface formed under the Sb-rich condition.

particles are easily formed during molecular beam epitaxy under In-stabilized surface conditions [5]. On the other hand, the surfaces of InSb films grown epitaxially on $\alpha$-Sn(111)($\theta$=5 BL)/InSb(111)*A* at 200 °C changed the structure with a film thickness of InSb, independent of the film thickness of $\alpha$-Sn. Below and above ~5 BL thickness of InSb the surface exhibited a (2×2) structure and the (2×6) reconstructed structure characteristic of (111)*A*-type, respectively, under the Sb-rich condition. In Figs. 1(b) and 1(c), the (2×2) and the (2×6) RHEED patterns are shown, respectively. The origin of the (2×2) will be confirmed below. From these results it appears that the as-grown InSb{111}*A*,*B* films receive the polarity of InSb{111}*A*,*B* used as substrates, although a nonpolar substance of $\alpha$-Sn exists between the overlayer and the substrate.

TABLE I. Comparison of AES peak height ratios of Sb(*MNN*)/In(*MNN*) from InSb films grown on $\alpha$-Sn/InSb(111)*B* and from homoepitaxially treated InSb(111)*B* substrates.

| | Sb(*MNN*)/In(*MNN*) | |
|---|---|---|
| InSb(111)*B* surface structures | InSb grown on $\alpha$-Sn(3 BL)/InSb(111)*B* | Homoepitaxially grown InSb |
| In-stabilized (3×3) | 0.74 | 0.89 |
| Sb-stabilized (2×2) | 1.24 | 1.21 |

In order to make it clear what has caused such a polarity alternative, we performed an EELS depth analysis for the $\alpha$-Sn(111)($\theta$=3 BL)/InSb{111}*A*,*B* substrates. Shown in Fig. 2 are the representative EELS spectra for $\alpha$-Sn(111)($\theta$=3 BL)/InSb(111)*B*. The principal transitions in this figure are due to excitations of Sb and Sn 4*d* core levels to the corresponding conduction bands. For both the Sb and Sn 4*d* spectra, there was a very slight shift to the higher energy side with an increase of the primary incident beam energy. Further interesting evidence is that the peak height ratio of Sb to Sn increases with decreasing the incident beam energy. Hence, the result shown in Fig. 2 reveals that a significant amount of Sb is accumulated at the $\alpha$-Sn surface layers, resulting in Sb segregation, and that dilution of the Sb in the $\alpha$-Sn films occurs. For $\alpha$-Sn(111)($\theta$=3 BL)/InSb(111)*A*, EELS spectra other than those for Sn were not observed, which indicates that the $\alpha$-Sn surface is clean. These results are also supported by the RHEED patterns obtained from two $\alpha$-Sn substrates. For $\alpha$-Sn(111)($\theta$=3 BL)/InSb(111)*A* the (3×3) pattern is observed, the existence of which assures us of the cleanliness of the $\alpha$-Sn(111) surface [3,4], and for $\alpha$-Sn(111)($\theta$=3 BL)/InSb(111)*B* the (1×1) pattern is observed, the emergence of which is possibly due to the segregation of Sb at the $\alpha$-Sn surface. Increasing the $\alpha$-Sn film thickness (>3 BL), the $\alpha$-Sn(111)/InSb(111)*A* surface continues to keep the (3×3) reconstruction in the initial surface and the $\alpha$-

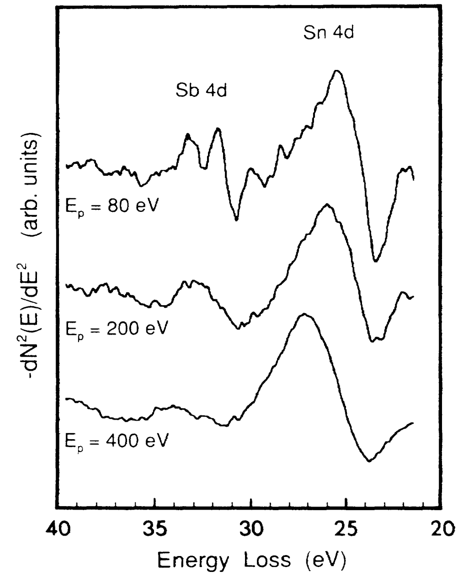

FIG. 2. EELS spectra recorded on $\alpha$-Sn(111)/InSb(111)*B*-(2×2) in the second derivative mode of the energy distribution *N*(*E*). $E_p$ is the primary incident beam energy.

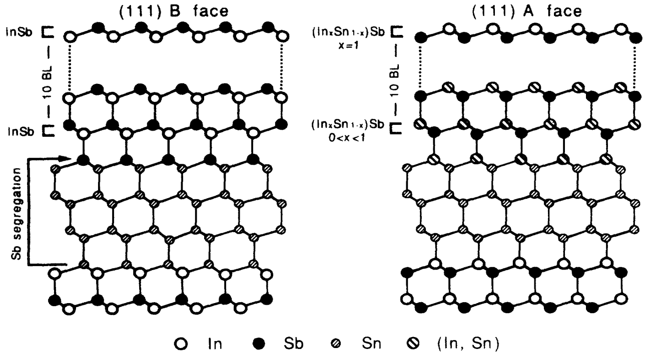

(a) InSb(111)B on α-Sn/InSb(111)B (b) InSb(111)A on α-Sn/InSb(111)A

FIG. 3. Schematic views in the $(\bar{1}10)$ plane of the InSb{111}*A*,*B*/α-Sn(111)/InSb{111}*A*,*B* system. (a) InSb-(111)*B* on α-Sn(111)/InSb(111)*B*. Note that Sb-Sn bonds are present at the InSb/Sn interface. (b) InSb(111)*A* on α-Sn(111)/InSb(111)*A*. Note that the intermixing layers of $(In_xSn_{1-x})Sb$ $(0 < x < 1)$ are present at the InSb/Sn interface region.

Sn(111)/InSb(111)*B* surface begins to exhibit the (3×3) from above 5 BL thick. Results for both the EELS and RHEED experiments show that Sb can segregate to the surface of the thinner (< 5 BL) α-Sn film for InSb(111)*B* substrate only.

It is known that in combinations of InSb with Au, Al, and Cu, Sb segregates to these metal surfaces [6]. Since Sb has five valence electrons it would be triply bonded to three atoms in the metal surfaces, leaving a lone pair state at the surface. Such a surface is expected to become highly stable. Similar structural models have been proposed for the As- and Sb-terminated (111) surfaces of Si and Ge, all of which exhibit (1×1) surface periodicities [7–10]. The EELS result for the α-Sn(111)/InSb(111)*B* system suggests that during the α-Sn overgrowth Sb moves to the growth front to form the α-Sn(1×1) surface, while leaving the epitaxially grown α-Sn film behind. Given in a part of Fig. 3(a) is a possible model for the heterojunction of α-Sn(111) with InSb(111)*B*. The Sb is detected up to 5 BL thick of α-Sn, which elucidates that the segregation of Sb is limited in a kinetic (nonequilibrium) process of this system; as the α-Sn films become thicker (> 10 BL), the Sb becomes difficult to segregate to the growing α-Sn surface. As a result, the surfaces of the InSb films grown on the Sb-free α-Sn surface always become of (111)*A* type. As predicted from these results, between 5 and 10 BL thick, an admixture of the *A*-type and the *B*-type region dominates the as-grown InSb film surfaces; naturally the area of the *A*-type surface enlarges with an increase of the α-Sn film thickness.

An onset of the *A*-type surface in the InSb/α-Sn(111)/InSb(111)*A* system begins with the InSb growth above 5 BL thick, independent of a film thickness of α-Sn. This is incompatible with the results for the GaAs/Si, Ge(111) systems; GaAs grows on Si(111) with the (111)*B* orientation [11,12] and on Ge(111) with both Ga-Ge and As-Ge bonds at the interface [12]. To address the question of how the formation of the interface between the grown InSb(111)*A* and the α-Sn film is initiated, we measured the AES peak intensities as a function of InSb film thickness. As can be seen in Fig. 4, all the signals change nearly exponentially with a positive slope for InSb and with a negative slope for 5 BL α-Sn. The AES intensities of the In and the Sn lines, however, are indicative of lower decay (dash-dotted line) and higher rise (broken line), respectively, than the corresponding (solid) curves calculated on the basis of an ideal interface model, such as (10 BL In-Sb)/(5 BL Sn-Sn). These deviations are probably due to interdiffusion between In and Sn, presumably to form intermixing layers of $(In_xSn_{1-x})Sb$ $(0 < x < 1)$. This seems reasonable by the findings that the thinner ( < 5 BL) InSb film surface does not exhibit the (2×6) reconstruction characteristic of the *A*-type surface but the (2×2) structure [Fig. 1(b)] and also by the following additional evidence; when only In was deposited on α-Sn(111)($\theta = 5$ BL)/InSb(111)*A* at room temperature, the RHEED pattern showed the presence of an incommensurate phase that suggested an intermixture of In with Sn, while Sb deposition on the identical substrate resulted in the growth of an amorphous phase composed of Sb. This means that Sn is more strongly bonded to In than Sb. The value of $x$ in $(In_xSn_{1-x})Sb$ decreases with increasing the film thickness of growing InSb. The pure *A*-type surface structure corresponds to $x = 1$. As a result, we reach a (111)*A* growth orientation onset model in the InSb/α-Sn(111)/InSb(111)*A* system, as shown in Fig. 3(b).

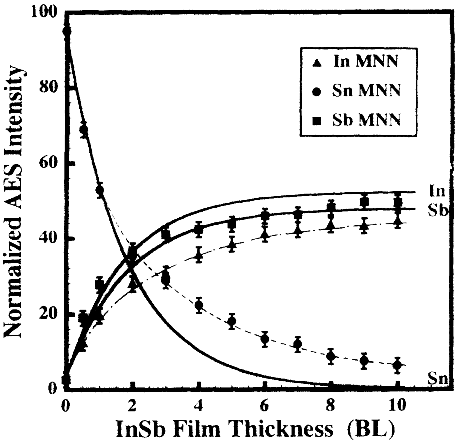

FIG. 4. Auger peak intensities for the In, Sb, and Sn *MNN* lines plotted as a function of InSb film thickness on the α-Sn(111)/InSb(111)*A* substrate at 200 °C. Solid lines represent the intensities expected for the biatomic layer-by-layer InSb(111)*A* growth on an abrupt interface. Deviations from the solid lines are indicative of interdiffusion between In and Sn.

In conclusion, we have successfully fabricated the InSb{111}*A*,*B*/$\alpha$-Sn(111)/InSb{111}*A*,*B* heterostructure by molecular beam epitaxy. In this heterostructure, the surface polarity of the epitaxially grown InSb{111} films can be controlled well by varying a film thickness of $\alpha$-Sn for InSb(111)*B* and that of growing InSb for InSb(111)*A*. The $\alpha$-Sn film thickness dependence of the surface polarity is due to Sb which segregates to the $\alpha$-Sn surface from the InSb(111)*B* substrate. On the other hand, thick InSb films ($>5$ BL) on $\alpha$-Sn(111)/InSb(111)*A* always grow with the *A*-type surface, although the thinner films ($<5$ BL) lead to the formation of the intermixing phase of $(\mathrm{In}_x\mathrm{Sn}_{1-x})\mathrm{Sb}$ ($0<x<1$). These findings will offer us a good opportunity to fabricate a polarity-controlled polar-nonpolar-polar heterojunction device.

We would like to acknowledge helpful discussion with A. Ohtake, S. Okamoto, T. Nakada, K. Yamamoto, J. Nakamura, and M. Iwai, throughout this work. This work was supported by a Grant-in-Aid for Scientific Research on Priority Areas "Crystal Growth Mechanism in Atomic Scale" (No. 03243107) from the Ministry of Education of Japan.

---

*Present address: Optoelectronics Research Laboratories, NEC Corporation, 34 Miyukigaoka, Tsukuba 305, Japan.

[1] J. Bohr, R. Feidenhans'l, M. Nielsen, M. Toney, R. L. Johnson, and I. K. Robinson, Phys. Rev. Lett. **54**, 1275 (1985).

[2] T. Nakada and T. Osaka, Phys. Rev. Lett. **67**, 2834 (1991).

[3] T. Osaka, H. Omi, K. Yamamoto, and A. Ohtake, Phys. Rev. B (to be published).

[4] Y. Kasukabe, M. Iwai, and T. Osaka, Jpn. J. Appl. Phys. **27**, L1201 (1988).

[5] T. Nakada, T. Ikeda, M. Yata, and T. Osaka, Surf. Sci. **222**, L825 (1989).

[6] D. M. Hill, F. Xu, Z. Lin, and J. H. Weaver, Phys. Rev. B **38**, 1893 (1988); Yoram Shapira, F. Boscherini, C. Capasso, F. Xu, D. M. Hill, and J. H. Weaver, *ibid.* **36**, 7656 (1987); F. Boscherini, Y. Shapira, C. Capasso, C. Aldao, M. del Giudice, and J. H. Weaver, *ibid.* **35**, 9580 (1987); F. Boscherini, Y. Shapira, C. Capasso, and J. H. Weaver, *ibid.*, **35**, 8022 (1988).

[7] R. D. Bringans, R. I. G. Uhrberg, R. Z. Bachrach, and John E. Northrup, Phys. Rev. Lett. **55**, 533 (1985).

[8] J. R. Patel, J. Zegenhagen, P. E. Freeland, J. A. Golovchenko, and D. M. Chen, J. Vac. Sci. Technol. B **7**, 894 (1987).

[9] K. J. Wan, W. K. Ford, and J. C. Hermanson, Surf. Sci. **268**, L253 (1992).

[10] Gerhard Meyer, Bert Voigtländer, and Nabil M. Amer, Surf. Sci. **274**, L541 (1992).

[11] J. R. Patel, P. E. Freeland, M. S. Hybertsen, and D. C. Jacobson, Phys. Rev. Lett. **59**, 2180 (1987).

[12] R. D. Bringans, M. A. Olmstead, R. I. G. Uhrberg, and R. Z. Bachrach, Phys. Rev. B **36**, 9569 (1987).

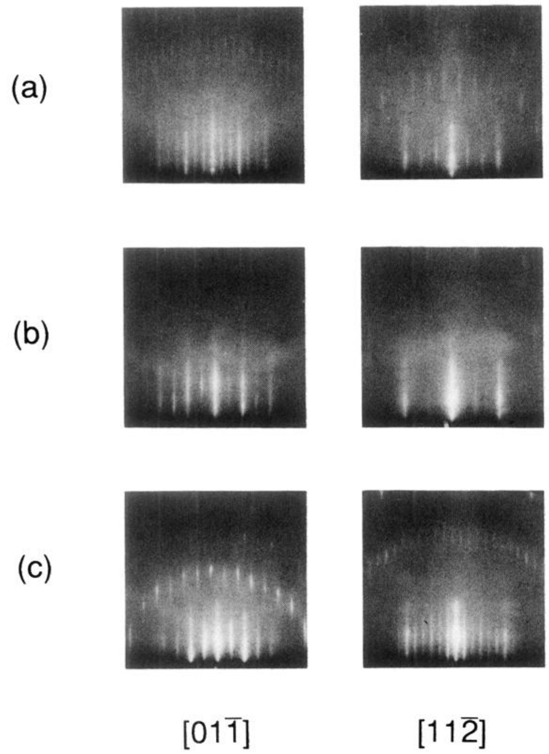

FIG. 1. RHEED patterns obtained by deposition of In and $Sb_4$ fluxes onto the $\alpha$-Sn(111)/InSb{111}*A*,*B*-(2×2) substrates at 200 °C. (a) The (3×3) reconstruction showing a *B*-type surface formed under the In-rich condition. (b) The (2×2) structure corresponding to the intermixing layers of $(In_xSn_{1-x})Sb$ formed under the Sb-rich condition. (c) The (2×6) reconstruction for an *A*-type surface formed under the Sb-rich condition.